

# **EFFECT OF OXIDATION IN AMBIENT AIR ATMOSPHERE ON THERMOPHYSICAL PROPERTIES OF ZIRCONIUM ALLOY<sup>1</sup>**

I.I. Petrova<sup>2</sup>, V.E. Peletsky<sup>2</sup>, B.N. Samsonov<sup>2,4</sup>, A.V. Nikulina<sup>3</sup>, N.B. Sokolov<sup>3</sup>,  
L.N. Andreeva-Andrievskaya<sup>3</sup>

---

<sup>1</sup> Paper presented at the 14 Symposium on Thermophysical Properties,  
June 25-30, 2000, Boulder, Colorado, U.S.A.

<sup>2</sup> Thermophysical institute of extremal states, United Institute for High  
Temperatures, Izhorskaya 13/19, 127412 Moscow, Russia.

<sup>3</sup> State Scientific Center of Russian Federation, VNIINM, Rogova 5a, 123060  
Moscow, Russia.

<sup>4</sup> To whom correspondence should be addressed

## ABSTRACT

The results of an experimental study of the effect oxidation on temperature dependence of heat capacity and spectral emissivity (for the wavelength of  $0.65\mu\text{m}$ ) of the zirconium alloy for nuclear reactors ( $\sim 1.3$  mass % Sn,  $\sim 0.3$  mass % Fe,  $\sim 1$  mass % Nb) are presented. The subsecond resistive pulse heating technique had been used. The samples were heated in ambient air atmosphere by single and multiple cyclic pulses.

KEY WORDS: heat capacity; oxide; spectral emissivity; subsecond resistive pulse heating; zirconium alloy.

## 1. INTRODUCTION

The zirconium based alloys are used in nuclear reactors for the envelopes of fuel elements and other components. For safety analysis of nuclear reactors, the accident situation must be examined when temperature of fuel elements is dramatically increases up to the melting point. So, it is necessary to have the exact data on thermophysical properties of zirconium alloys at high temperatures for nuclear fuel elements behavior prediction.

At previous paper [1], we have described the use of subsecond pulse technique for study of Zr-0.01Nb-0.003Fe-0.013Sn alloy the thermophysical properties in an inert (argon) atmosphere. At present work the experiments have been carried out at the conditions similar to probable accident conditions - rapid heating and an oxidizing ambient atmosphere. As it may be seen from our results described below, the oxidizing atmosphere makes the noticeable effect on the properties of the zirconium alloy at high temperatures and especially at the temperature range of the  $\alpha$ - $\beta$  phase transition. The

samples used in experiments were made from commercial tubes of nuclear fuel elements envelopes.

## 2. METHOD OF MEASUREMENTS

The technique of subsecond pulse resistive heating [2] of samples with high density direct current ( $\sim 5000 \text{ A/cm}^2$ ) from room up to melting temperature with the rate of about  $1000 \text{ K/s}$  was used. The length of studied tubular samples was  $\sim 75 \text{ mm}$ ; their external diameter was  $\sim 9.1 \text{ mm}$ ; internal diameter was  $\sim 7.7 \text{ mm}$ . The distance between two probes in the central part of the sample, where the voltage drop was measured, was equal to  $10 \text{ mm}$ . The blackbody model for measurement of the true temperature was made with a rectangular slit,  $20 \text{ mm}$  long and  $1 \text{ mm}$  wide. The model with the parameters like these is good enough and it ensures an isothermic field along the working section [3] during the heating with rate mentioned above. The effective emissivity of such a blackbody was found experimentally and equal to  $0.89$ . Two high-speed photoelectric pyrometers (both with wavelength of  $0.65 \text{ }\mu\text{m}$ ) synchronous measured temperatures of the sample during experiment. One of them measured the brightness temperature of the surface (its lower limit of measurements was about  $1600 \text{ K}$ ), the other one - the true temperature of the blackbody model (its lower limit was  $900 \text{ K}$ ). All primary parameters (the electrical current  $I$ , the voltage drop along the working section  $U$ , true temperature  $T_{tr}$ , and brightness temperature  $T_{br}$ ) were measured using an A/D-converter with a sample rate from  $100$  up to  $1000 \text{ samples/s}$ .

The heat capacity  $C_p$  and the spectral emissivity  $\varepsilon_\lambda$  (for wavelength  $\lambda=0.65 \text{ }\mu\text{m}$ ) have been calculated with the following expressions:

$$C_p = \frac{UI - q_r}{m \left( \frac{dT}{d\tau} \right)_h} \quad (1)$$

$$\ln \varepsilon_\lambda = \frac{c_2}{\lambda} \left( \frac{1}{T_{tr}} - \frac{1}{T_{br}} \right) \quad (2)$$

In these expressions  $m$  is the mass of the central working section of the sample,  $C_2=1.4388 \times 10^{-2}$  m·K is the second constant in Planck's law,  $(dT/d\tau)_h$  is the rate of heating,  $q_r$  is a correction for the radiation heat losses, and  $\lambda$  is the wavelength of pyrometers.

### 3. RESULTS OF MEASUREMENTS

#### 3.1. Heating and Cooling Thermograms

There were performed the number of experiments for four samples. The first three were heated by a single pulse up to 1700, 1900, 2100 K respectively, and the fourth was heated up to 1900 K five times and cooled down to room temperature after every pulse. The increase of weight due to an oxidation was measured after every experiment.

Fig. 1 shows the dependences of  $T_{tr}=f(\tau)$  (curve 1) and  $T_{br}=f(\tau)$  (curve 2) which have been measured at the experiment with single pulse heating up to 1900 K in an air atmosphere; the part of this figure (heating only) is shown in Fig. 1a. The heating time in this case was about 1.5 sec.; the time of cooling down to  $T_{tr}=900$  K was about 20 sec. The difference between these thermograms and the thermograms, which have been obtained in the previous study for heating in an argon atmosphere is the presence of the low rate cooling section for the first ten second of cooling, in temperature range 1900 – 1600 K. The reason of it may be an exothermic (heat-emission) oxidation reaction

which takes place in an air atmosphere. We can see also the other unusual effect, namely, the decrease of the difference between the true and the brightness temperatures for the cooling section and even the overcoming the last one. It may be explained by more active oxidation of the outward surface of the tube in comparison with inward one. The other reason of this effect may be an appearance inside the tube in a reaction zone some fine dispersed particles of oxides of fusible elements, which can evaporate from the alloy. As concentration of the particles in closed volume (into the tube) is higher than outside it, the extinction of the blackbody radiation at measurement of the true temperature may be more than the extinction of the surface radiation. Though this reason is only supposition, it must be noted that a white deposition of the very small particles on the upper current feed have been discovered after experiment at opening of the vacuum chamber. Of course, it is possible that there are some other reasons, for example, a more heat transfer from the inner wall of the tube to the convective air flow in comparison to heat transfer from its outward wall.

After the single pulse heating and subsequent cooling in an air atmosphere on a cross section of the sample some components can be marked out: a non-stoichiometric oxide film on the tube surfaces, a diffusion layers near the surfaces – oxygen solid solution in the alloy with variable concentration along the profile, and the pure alloy (without oxygen) which still takes the central part of the sample cross section. For a system like this we can see two breaks (marked by the circles) on the thermograms (Fig. 1, 1a). The first one at  $T_{tr} = 1100-1200$  K is the  $\alpha-\beta$  transition in the alloy and in adjoining oxygen solid solution diffusion layer. The small second break at  $T_{tr} \cong 1300$  K is the oxide film phase transition from monoclinic to tetragonal lattice [4]. It is not very expressive at the heating region. As we can see from Fig. 1 and 1a, the  $\alpha-\beta$  phase

transition temperature is higher at heating stage in comparison to cooling one. It can be explained by the delay in a new phase nucleation at high rate processes and by the significant difference between the heating and cooling rates.

Fig. 2 shows the thermograms of the true (1) and the brightness (2) temperatures of the zirconium alloy sample heated by a single pulse in an air atmosphere up to  $T_{tr}=2100$  K. As we can see, the character of cooling section thermogram depends on the value of maximum temperatures. There is even some temperature rise after switching off an electrical current. This temperatures rise is explained by more generation of heat at an oxidation, than in the case, when the sample was heated up to 1900 K.

The experiments with 5 heating-cooling cycles on the single sample were carried out and the true temperature thermograms are shown in Fig. 3. For every cycle the sample heated up to  $T_{tr}=1900$  K and cooling down to the room temperature. The first pulse thermogram is significantly differ for the cooling stage from the following ones. The initial sample surface was “clean“ (not oxidized), and after the switching off heating stop there was intense oxidation with heat generation, as it is seen from the low cooling rate for the first thermogram (1). After the first pulse the sample was covered with non-stoichiometric oxide film. For the second pulse and the following ones the sample oxidation process was less intense, as it is seen from cooling rates. After an every cycle of pulse heating-subsequent cooling the color of the sample surface becomes lightly, i.e., oxide film turns to more stoichiometric.

The  $\alpha$ - $\beta$  phase transition breaks on the thermograms (Fig. 3) become more smooth with every next heating pulse, i.e., the  $\alpha$ - $\beta$  phase transition temperature range grows due to increasing of diffusion layers thickness.

The microhardness  $H_{50}$  distributions along the cross section of the tube wall for three samples are shown in Fig. 4. The first sample was heated by a single pulse up to  $T_{tr} = 1900$  K (1), the second one - up to  $T_{tr} = 2100$  K (2), and the third had five repeated cycles pulse heating up to  $T_{tr} = 1900$  K and subsequent cooling (3). As it can be seen from Fig. 4, the microhardness near the outer surface of a tube wall is higher, than at the inner one after a single pulse heating. For a multiple cyclic pulse heating the microhardness near the both surfaces of tube wall is the same. The increase of the microhardness in the central part of a tube wall means that the entire tube wall after five heating cycles was involved in oxygen dissolution.

### **3.2. Heat Capacity**

The heat capacity is the property, which is most sensitive to phase and structural transitions in materials. Some small breaks of the presented thermograms of zirconium alloy, heated in an air atmosphere, mean the significant changing of the heat capacity. The temperature dependences of the heat capacity for various cyclic heating in an air atmosphere are shown in Fig. 5. For the first heating (curve 1), when the sample structure and composition are practically initial, the first heat capacity peak is around  $T_{tr} = 1170$  K and it corresponds to the  $\alpha$ - $\beta$  phase transition of not oxidized alloy. With every next heating, as the oxygen concentration in alloy is rising, the height first peak is decreasing and for the same time its temperature range is expanding. The second small peak on curve (1) is near  $T_{tr} = 1400$  K (see also Fig. 1a) and it may be associated with heat consumption for dissolution of a thin oxide film. This film was arisen at the heating stage from oxygen, adsorbed by the specimen surface. After the first heating-cooling cycle a dark-colored film of non-stoichiometric oxide has covered the sample in near-surface diffusion layers the concentration of dissolved oxygen is high, as for the first

heating the initial sample surface has the great absorbability and can absorb more oxygen than for following cycles of heating. The augmentation of mass of the sample after the experiments indicates it clearly: the increase of mass after first heating was about three times greater than after the following ones. So, the second peak on the curve (2), corresponding to the  $\alpha$ - $\beta$  phase transition in near-surface layer, takes place at high temperature ( $T_{tr} = 1620$  K). It must be noted that oxidizing process for subsecond pulse experiments takes place mainly at cooling stage, as it much slower. For the third heating and following ones a rich solid solution at near-surface layers is transforming to oxide, and on the heat capacity curve the second peak at  $T_{tr} = 1620$  K is the oxide structural transition from the monoclinic to the tetragonal modification. In according to Ref. [4] the temperature of equilibrium transition a monoclinic structure to tetragonal is  $T_{tr} = 1470$  K for pure non-stoichiometric zirconium oxide, and it is not far from our results. With every next following heating the height of the second peak increases, that means the growth of an oxide film thickness, and at the same time the height of the first peak ( $\alpha$ - $\beta$  phase transition in the alloy with dissolved oxygen) decreases, and it's temperature range expands. With all this going on, the starting temperature of  $\alpha$ - $\beta$  phase transition stays the same as for pure alloy ( $T_{tr} = 1070$  K), until the oxygen reaches the center of tube wall. The temperature dependencies of heat capacity for the same alloy in an argon atmosphere for cyclic pulse heating (5 pulses also) are shown in Fig. 6 for comparison. There is significant difference in the behavior of the alloy heat capacity for heating in an air atmosphere and in an inert one (Fig. 5, 6).

The data on the heat capacity for the first heating in an air atmosphere for 3 samples are shown in Fig. 7. An experimental data good reproducibility for the phase transition area can be seen.



### 3.3. Spectral Emissivity.

There is significant difference between the absolute values and temperature dependences of the alloy spectral emissivity  $\varepsilon_\lambda=f(T)$  for heating in an air atmosphere and in an inert one. It can be seen from Fig. 8, where the curves 1 and 2 concern to an air atmosphere experiments, and curve 3 to an argon one. Due to a presence of the oxide film on a sample surface in an air atmosphere heating, the emissivity  $\varepsilon_\lambda$  is significantly more then in an argon heating in the whole measured temperature range. At a rapid heating, the temperature dependence of  $\varepsilon_\lambda$  has an uncommon character with a pronounced maximum at  $T_{tr}=1700$  K, and it is in correlation with surface changes which take place during an oxidizing process. In all experiments with single heating the decrease of the temperature rate at  $T=1700$  K can be seen from the brightness temperature thermograms (Fig. 1a, curve 2). It may be associated with structural transformation in thin oxide film on the sample surface. The increase of  $\varepsilon_\lambda$  at  $T_{tr}>2000$  K (Fig. 8, curve 2) may be explained by intense oxidizing of the alloy and the formation of the oxide particles of the light fusible elements in the gas phase. At this conditions, the effective emissivity of blackbody decrease.

The temperature dependences of the spectral emissivity  $\varepsilon_\lambda$  for cyclic pulse heating (5 pulses) up to  $T_{tr}=1700$  K in an air atmosphere are shown in Fig. 9. For the first pulse, the emissivity  $\varepsilon_\lambda$  growths from 0.64 at  $T_{tr}=1600$  K up to 0.7 at  $T_{tr}=1700$  K, than it decreases to 0.67 at  $T_{tr}=1900$  K. The maximal film growth takes place at the cooling stage, after the first heating, as it mentioned above. The sample surface are covered by a dark-colored oxide film after the first heating, so for the second pulse we have a high emissivity  $\varepsilon_\lambda$  in the whole measured temperature range. Abnormal high

values of the emissivity ( $\varepsilon_\lambda \geq 1$ ) in the region  $T_{tr}=1600-1700$  K for the second heating can be explained, most likely, by an understating of the measured true temperature at its measurement in the blackbody model inside the tube, according to the reasons mentioned before. The values of the spectral emissivity for an oxidized zirconium alloy for the third, fourth and fifth heating pulses practically are the same. In temperature range of  $T_{tr}=1600-1700$  K the emissivity is decreases from 0.75 to 0.6.

#### 4. CONCLUSION

The series of experiments have been carried out with the purpose of studying the influence of oxidizing environment (ambient air atmosphere) on thermophysical properties of zirconium alloy. The subsecond technique have been used for resistive heating of samples, which were made from the commercial envelops of the fuel elements of nuclear reactors. It is found out the significant differences in the results obtained in an air atmosphere and in the inert one at the same conditions. The reasons of it are both the oxide film generation on a sample surface and, just as, the oxygen diffusion and dissolution into the samples. The appearance of the second peak, that is more high temperature, on the heat capacity curve (in addition to the peak of  $\alpha$ - $\beta$  phase transition in the alloy), corresponded to the oxide film phase transition is the specific feature of heating in an air atmosphere. The position and the amplitude of the first and the second peaks are changed for every next heating pulse and correlated with a sample oxidizing dynamic. When the number of pulses grows, the amplitude of the first peak on the curve  $C_p=f(\tau)$ , correlated with  $\alpha$ - $\beta$  phase transition, decreases, and the peak width broadens. The increase of the concentration of an oxygen dissolved in alloy can explain it, just as the increase of the diffusion layer thickness. Absolute values of  $C_p$  in  $\beta$ -phase

increase with every next heating pulse, as the sample becomes more saturated by an oxygen.

The change of the temperature dependences of spectral emissivity at rapid heating in an air atmosphere correlates with oxidizing dynamic of the sample surface. As the number of heating pulses increases, the transformation of a dark, non-stoichiometric oxide film into the white, stoichiometric one, is accompanied by the decreasing of the emissivity  $\varepsilon_\lambda$  at the temperature  $T_{tr}=1700$  K. The absolute  $\varepsilon_\lambda$  values at heating in an air atmosphere are greater, than in argon one in the whole measured temperature range.

## ACKNOWLEDGMENTS

The work had been supported by the Russian Fondation for Basic Research (project № 99-02-18258).

## REFERENCES

1. V.E. Peletsky, I.I. Petrova, B.N. Samsonov, A.V. Nikulina, N.B. Sokolov, L.N. Andreeva-Andrievskaya, in *Proceeding of the Conference on Thermophysical Aspects of WWER-Type Reactor Safety*, Vol. 2, A.D. Efanov, ed. (Ministry of Russian Federation for Atomic Energy, Institute of Physics and Power Engineering, Obninsk, 1998), p. 162.
2. I.I. Petrova, and V.Ya. Chekhovskoi, *Teplofiz. Vys. Temp.* **26**: 271 (1988).
3. V.E. Peletskii, *High Temperature*. **37**: 123 (1999).
4. R.J. Ackermann, S.P. Garg, and E.G. Rauh, *J. of Amer. Ceramic Society*. **60**: 341 (1977).

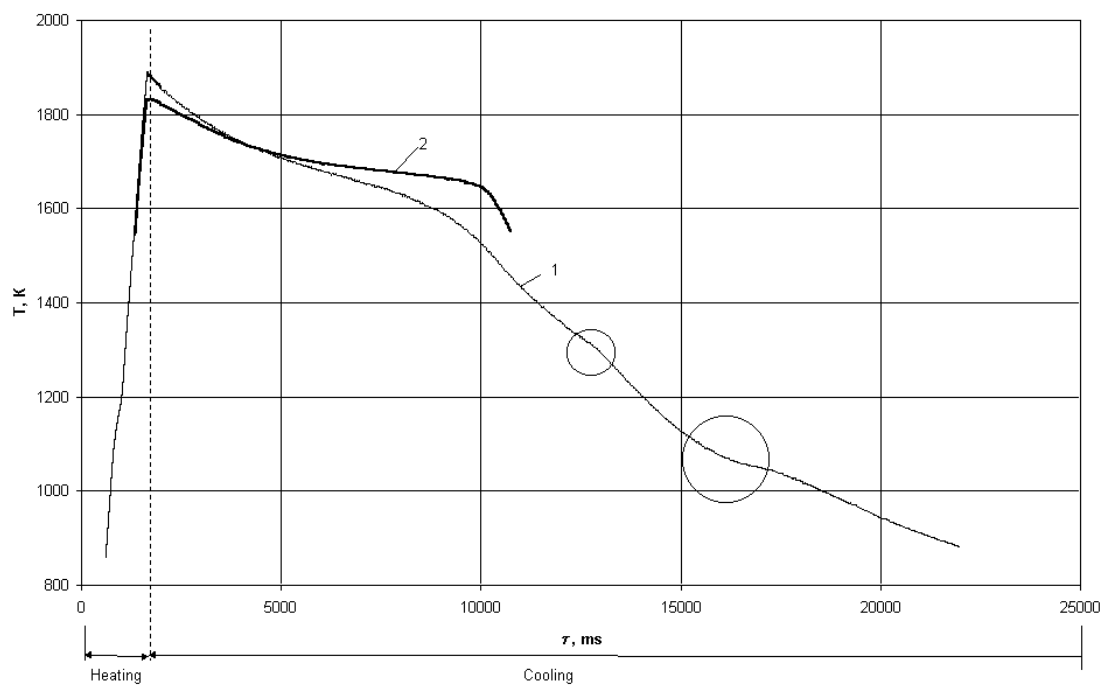


Fig.1 The true (1) and brightness (2) temperatures of a zirconium alloy at a single pulse heating up to  $T=1900$  K (heating-cooling).

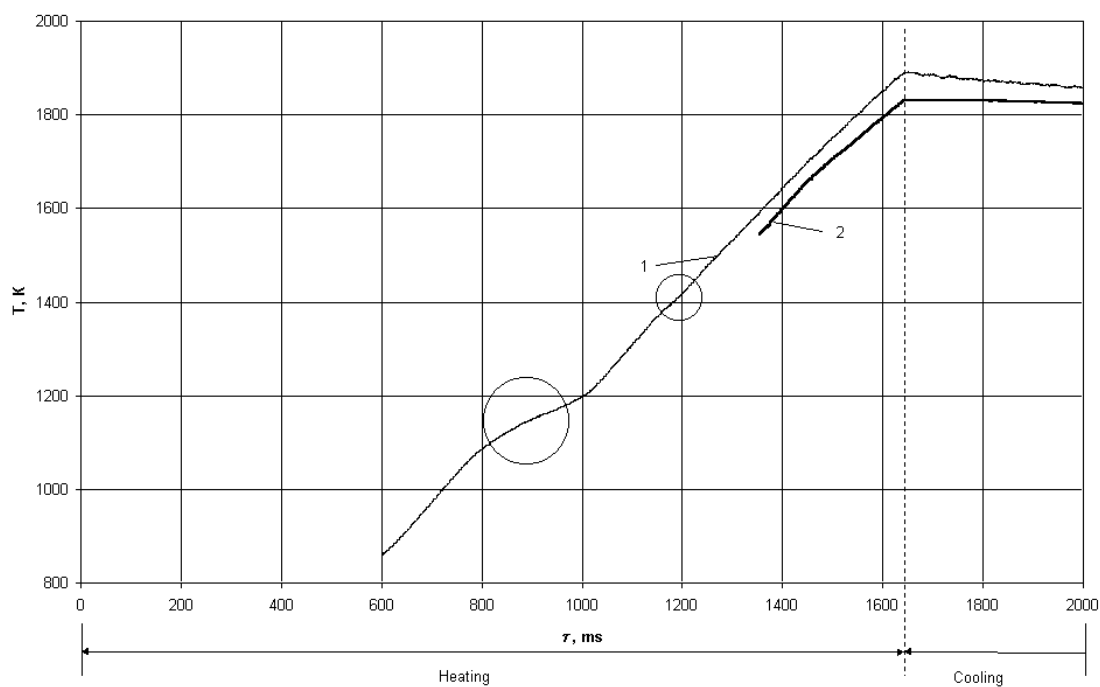


Fig.1a The true (1) and brightness (2) temperatures of a zirconium alloy at a single pulse heating up to  $T=1900$  K (heating).

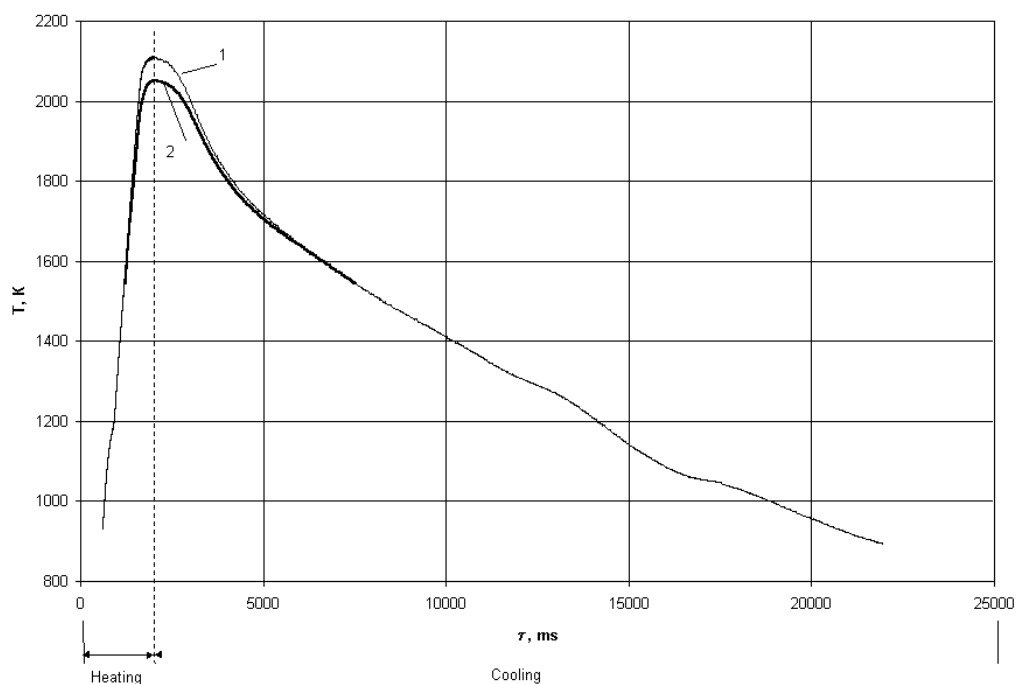


Fig.2 The true (1) and brightness (2) temperatures of a zirconium alloy at a single pulse heating up to  $T=2100$  K (heating-cooling).

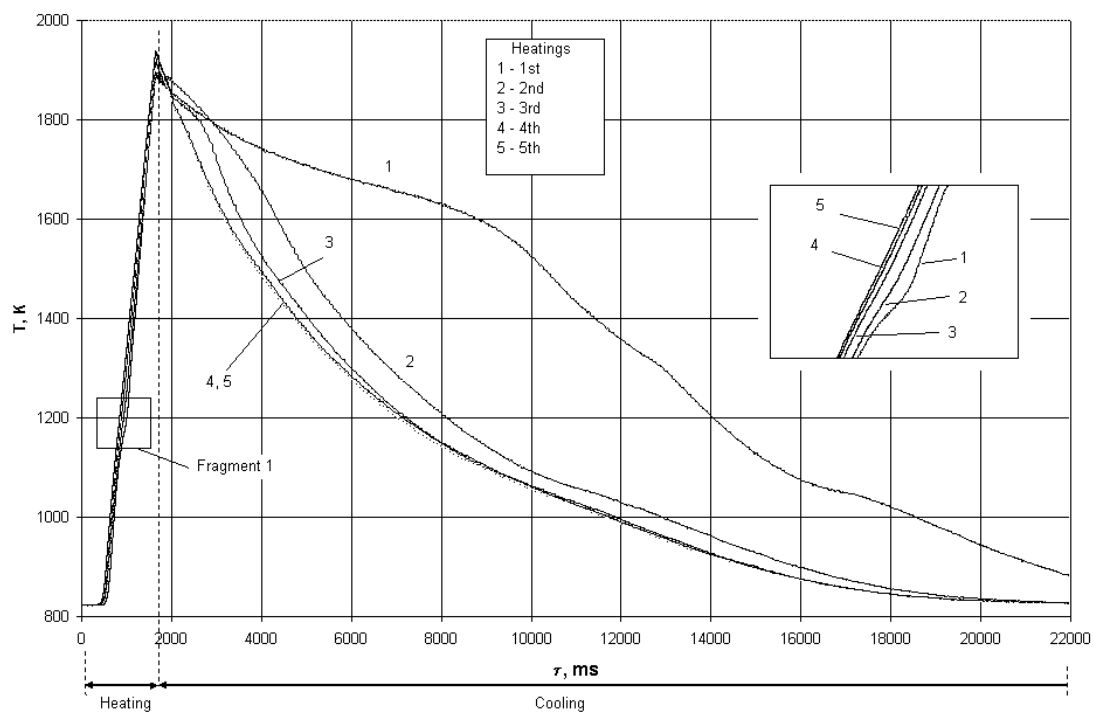


Fig. 3. The true temperatures of the zirconium alloy for the various cycles of pulse heating.

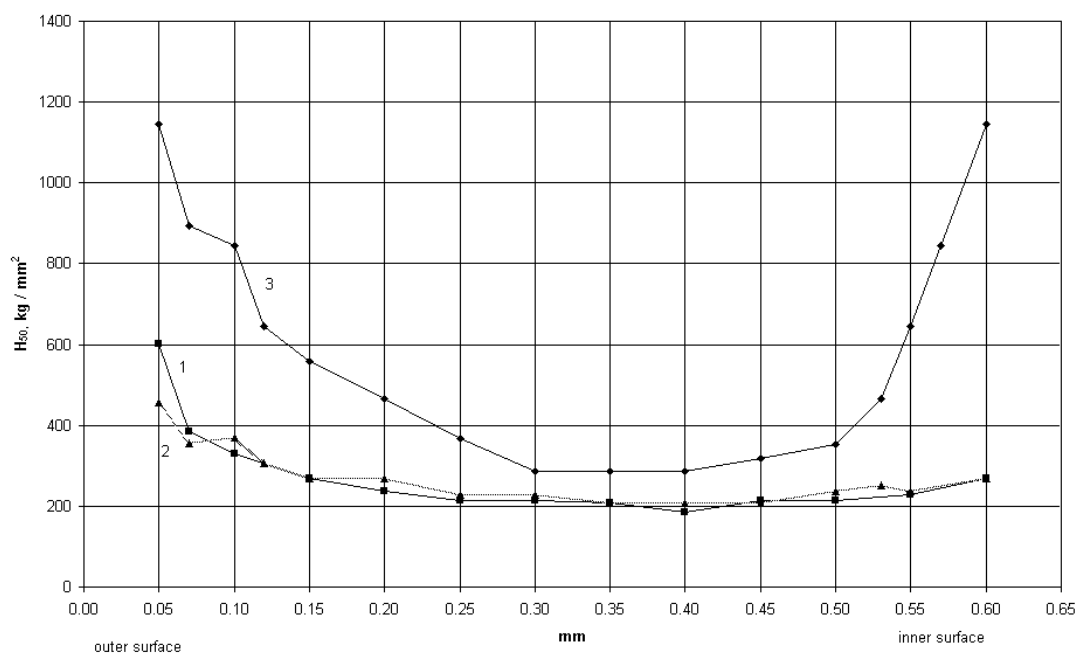


Fig. 4. Distribution of the microhardness H50 along the cross section of the tube wall after single pulse heating up to  $T=1900$  K (1);  $T=2100$  K (2); after repeated cycles heating (5 pulses) up to  $T=1900$  K (3).

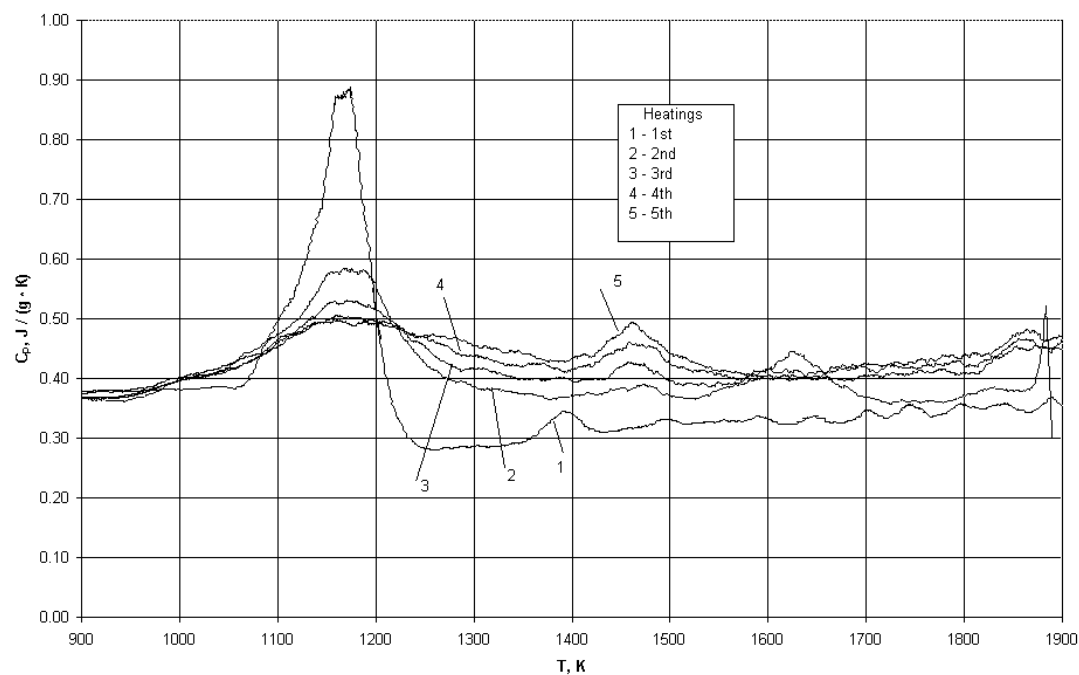


Fig. 5. The heat capacity at cyclic pulse heating in an air atmosphere.

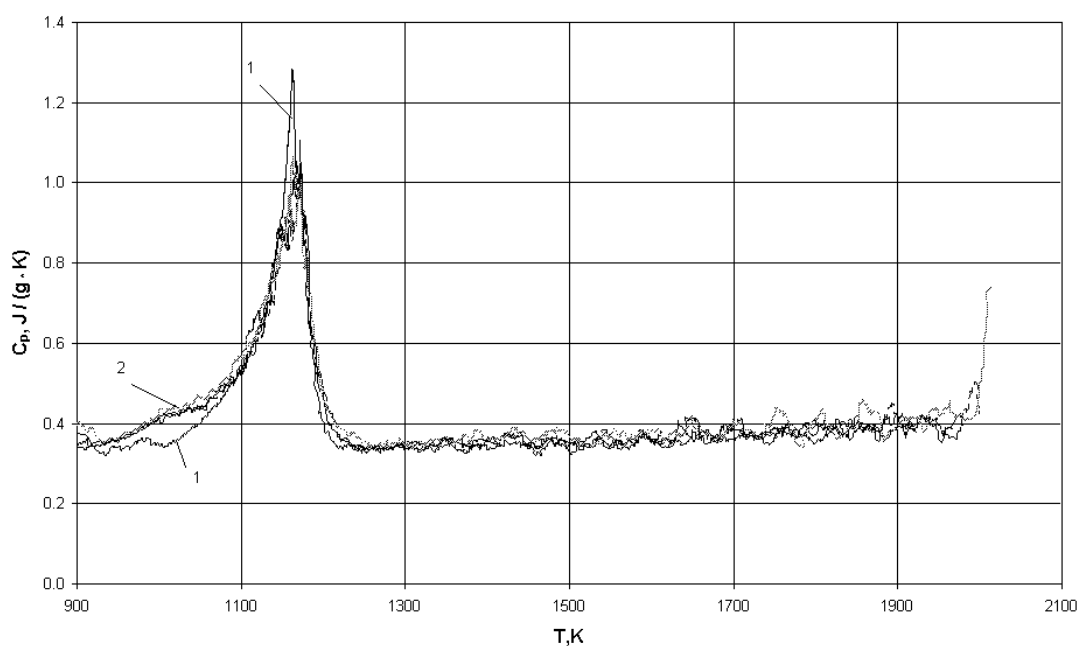


Fig.6 The heat capacity temperature dependence of a zirconium alloy at cyclic pulse heating in an argon atmosphere 1-first heating; 2-all the following ones

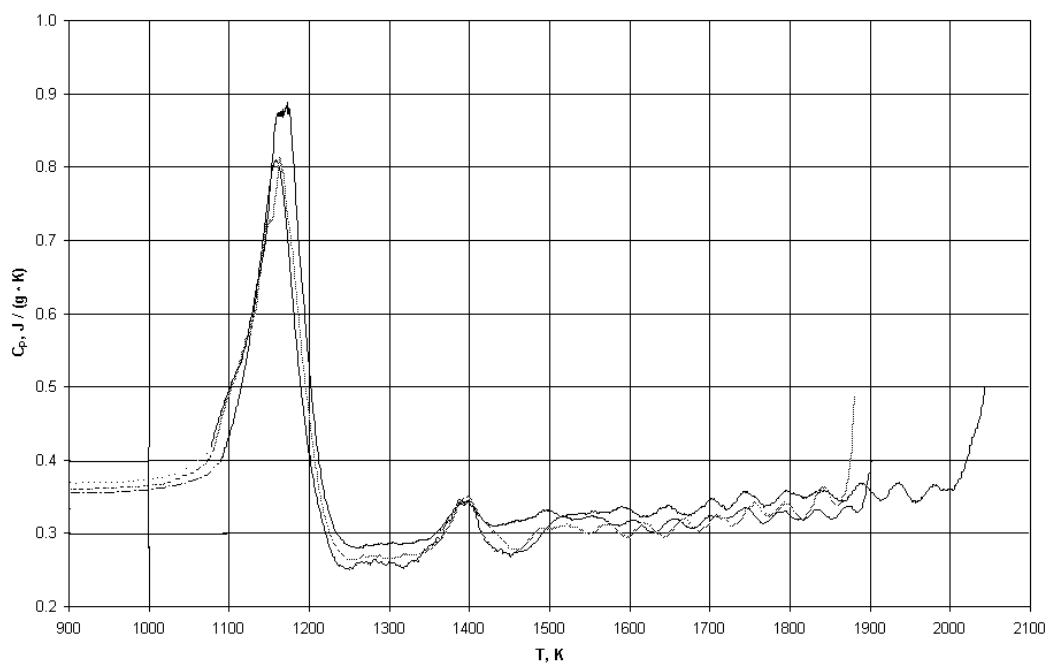


Fig. 7. The heat capacity of three various samples for the first heatings.

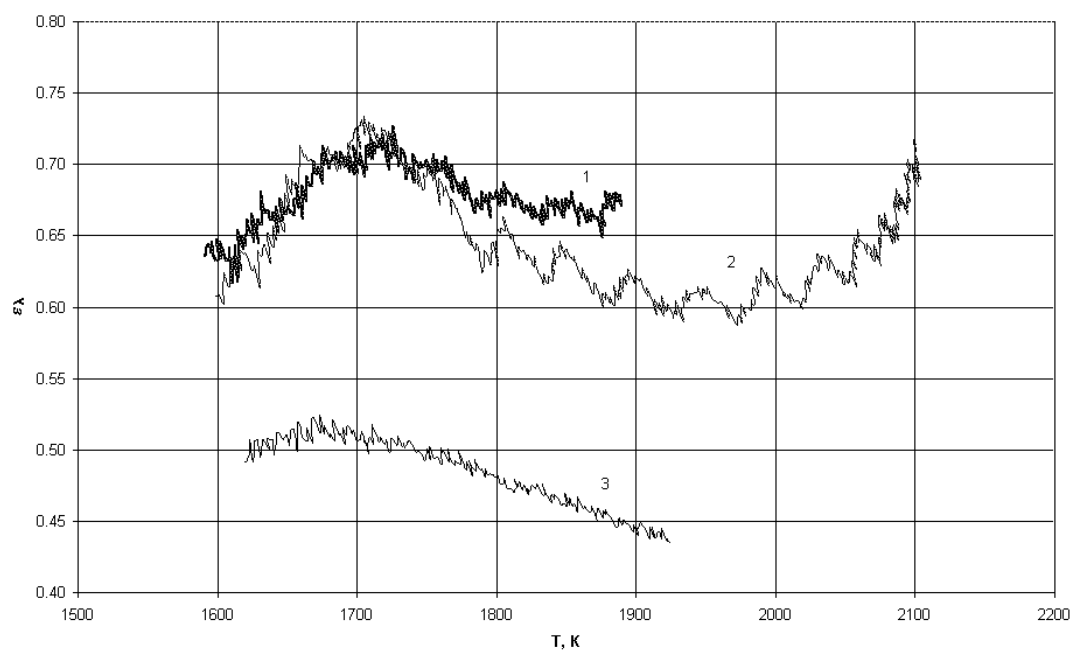


Fig. 8 Zirconium alloy spectral emissivity at the first heating in an air atmosphere (1, 2) and in an argon one (3).

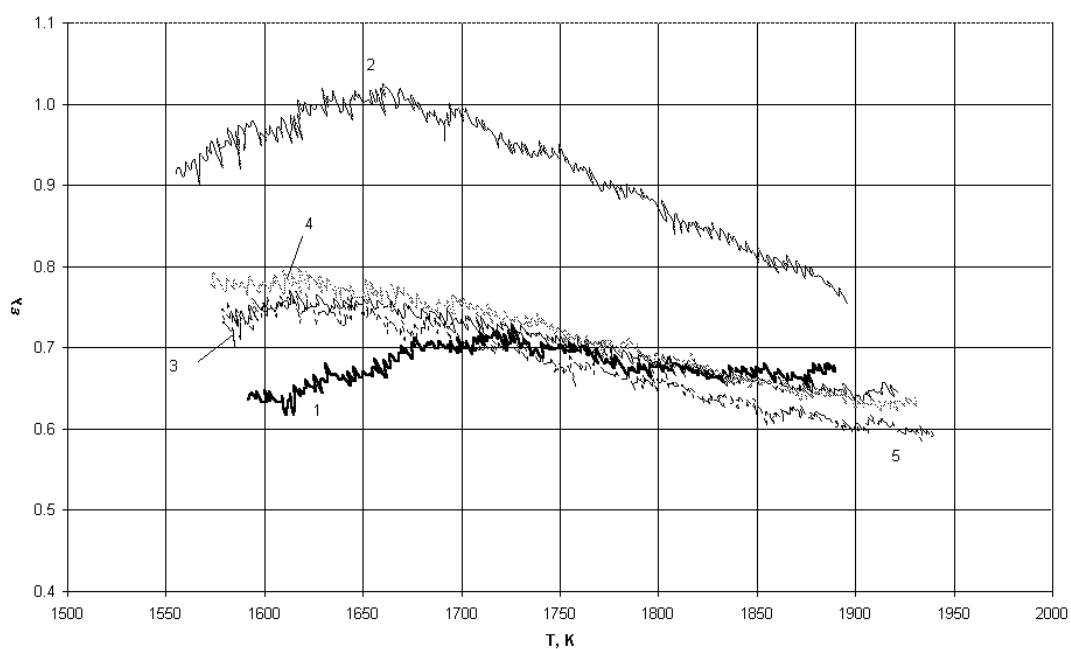


Fig. 9 Zirconium alloy spectral emissivity at the cyclic heating in an air atmosphere.